SUPPLEMENTARY MATERIALS

Supplementary Materials for

Stromal cell Protein kinase C-β inhibition enhances chemo-sensitivity in B cell malignancies and overcomes drug resistance

Eugene Park‡, Jingyu Chen‡, Andrew Moore‡, Maurizio Mangolini, Antonella Santoro, Joseph R. Boyd, Hilde Schjerven, Veronika Ecker, Maike Buchner, James C. Williamson, Paul J. Lehner, Luca Gasparoli, Owen Williams, Johannes Bloehdorn, Stephan Stilgenbauer, Michael Leitges, Alexander Egle, Marc Schmidt-Supprian, Seth Frietze and Ingo Ringshausen*.

‡ equal contribution
*Corresponding author. Email: ir279@cam.ac.uk

This file includes:

Materials and Methods

Primary cells and cell culture

After informed patients' consent and in accordance with the Helsinki declaration, peripheral blood was obtained from patients with a diagnosis of CLL, ALL, or MCL. Studies were approved by the local ethical committees of the Cambridgeshire Research Ethics Committee (07/MRE05/44), Technical University Munich (project number 1894/07), and the Institutional Review Board of the Erasmus MC. Peripheral blood mononuclear cells (PBMC) were isolated from heparinized blood samples by centrifugation over a Ficoll-Hypaque layer (PAN-Biotech). Malignant B cells were harvested and cultured in RPMI 1640 (Gibco), supplemented with 10% fetal calf serum (FCS) penicillin/streptomycin 50 U/ml, sodium-pyruvate 1mM, L-glutamine 2 mM, L-asparagine 20 mg/ml, 50 μM 2-mercaptoethanol , 10mM HEPES and MEM non-essential amino acids (Gibco). All primary mouse bone marrow stromal cell cultures were cultured in MEM Alpha + GlutaMAX medium (ThermoFisher Scientific) supplemented with 10% fetal calf serum, 10% horse Serum (StemCell Technologies) 10 μM 2-mercaptoethanol and 1% penicillin/streptomycin (Gibco).

Extraction of murine bone marrow stroma cells

All *in vivo* experiments were conducted in accordance with UK Home Office regulations (License P846C00DB). Murine bone marrow MSCs were established from femora and tibiae of 4 to 8 week-old mice. Bone marrow stroma cells were harvested from young female age-matched *Prkcb*$^{+/+}$ and *Prkcb*$^{-/-}$ by flushing the cavities of femora and tibiae with PBS. After filtration through a 70-μm filter and depletion of erythrocytes using a lysis buffer (BD PharmLyse; BD Biosciences), washed cells were either used further for experiments or cryopreserved.

Co-culture in vitro toxicity assay

Malignant B cells from CLL, ALL, or MCL patients co-cultured on murine BMSCs, CD14^{+}, or splenic follicular reticular cells (FRCs; gp38^{+}CD31^{-}) from PKC-β WT or PKC-β KO mice. Since PKC–β KO stroma grow marginally slower than WT, cell numbers were adjusted and BMSCs were seeded at equal concentrations of 2*10^{4} cells per well of a 96-well plate and incubated for 24 hours to allow for attachment. Subsequently, CLL, ALL, or

MCL cells were seeded at $2*10^5$ cells per well for monoculture and co-culture conditions and incubated for 24 hours. Enzastaurin (Sigma-Aldrich), sotrastaurin, bendamustine, idelalisib, midostaurin (Selleck Chemicals), venetoclax (LC Labs), fludarabine (Cayman Chemicals), ibrutinib (SYNkinase), dexamethasone, and vincristine sulfate (Sigma-Aldrich) were added at specified concentrations and incubated for up to 48 hours, prior to flow cytometric analysis (representative gating depicted in fig. S11A).

Generation of chimeric mice

Bone marrow from CD45.2$^+$ *Prkcb*$^{+/+}$, *Prkcb*$^{-/-}$, and CD45.1$^+$ B6.SJL-Ptprca Pepcb/BoyJ (Jackson Laboratories) age-matched mice were isolated and depleted of CD45$^-$ cells with purity of >95% confirmed by flow cytometry (muCD45 microbeads; Miltenyi Biotec). $3*10^6$ cells of purified bone marrow of respective CD45.2$^+$ *Prkcb*$^{-/-}$ purified-BM and CD45.1$^+$ B6.SJL-Ptprca Pepcb/BoyJ purified-BM were injected intravenously into respectively different CD45 recipients, post-irradiation (10 Gy) (i.e. CD45.1$^+$ BM into CD45.2 recipient and CD45.2$^+$ BM into CD45.1 recipient). CD45.2$^+$ *Prkcb*$^{-/-}$ BM was also injected into irradiated CD45.2$^+$ *Prkcb*$^{-/-}$ recipients as a control (Fig. 2). Chimerism was assessed by flow cytometry of CD45.1 and CD45.2 staining of peripheral blood withdrawn by tail vein bleeding (representative gating depicted in fig. S11B). Serum immunoglobulin isotype levels were assessed from peripheral blood using a mouse specific immunoglobulin isotype panel and subsequently analyzed and quantified using commercial software (LegendPlex Mouse Ig Panel, LegendPlex Analysis Software; Biolegend). Peritoneal fluid, peripheral blood, bone marrow, and spleen were harvested from respective animals and analyzed by flow cytometry. Chimeric mice of appropriate genotype upon confirmation of chimerism were injected with $40*10^6$ CFSE-labelled *TCL1*-tumor cells intravenously and $1*10^6$ cells injected intraperitoneally. Assessment of labeled CLL cells in peripheral blood was performed by flow cytometry.

Western blotting

After the specified time CLL cells were lysed in RIPA buffer and a total of 15 µg protein was separated by SDS-polyacrylamide gel electrophoresis, blotted to polyvinylidene difluoride (PVDF) membranes (Millipore) and probed with primary antibodies against BCL-X_L (Cell Signalling Technologies), BCL-2A1, β-actin (both Sigma-Aldrich), NOXA,

PUMA (both Abcam), BCL-2, BIM (both BD Biosciences), Mcl-1 (Santa Cruz Biotechnology).

RNA-sequencing and data analysis

CLL cells were cultured in mono-culture, or co-culture on murine BMSCs from WT or PKC-β KO mice for 12 hours. Primary CLL cells were seeded at 6 $x10^6$ cells on the top of 1 x 10^5 bone marrow MSCs per well of a 6 well plate. CLL cells were harvested for bulk RNA extraction and DNase treatment (RNA mini-prep kit, Sigma-Aldrich). Purity was confirmed by FACS analysis to be >95%. Human CLL cDNA libraries were prepared by using NEBNext Ultra Directional RNA Library Prep Kit for Illumina (New England Biolabs). Quality of cDNA libraries were determined using a Bioanalyzer High Sensitivity Chip (Agilent). Single-read sequencing was performed on the Illumina HiSeq 4000 platform at the CRUK Cambridge Institute Genomic Core. Stromal cDNA libraries were similarly synthesized and analyzed.

Sequencing data quality was assessed using the RSeQC package*(60)* and low quality reads and adapter sequences were removed using Trimgalore. Filtered data were aligned to the mm10 or hg38 reference genomes using RNA-STAR aligner*(61)* using the GENCODE Release 25 comprehensive GTF file with the following parameters: --outSAMtype BAM SortedByCoordinate --sjdbGTFfile annotation.gtf --outFilterType BySJout --outFilterMultimapNmax 50 --alignSJoverhangMin 1 --outFilterMismatchNmax 2 --outFilterMismatchNoverLmax 0.04 --alignIntronMin 20 --alignIntronMax 1000000 --alignMatesGapMax 1000000 --outSAMstrandField intronMotif. Quantification of gene expression was performed with HTSeq-0.11.0 *(62)* against the comprehensive gene annotation files from GENCODE (m14 and v25, for mouse and human genomes, respectively). Differential expression analysis was performed using DESeq2*(63)*, controlling for differences between patient samples. To generate the heat-map shown in Fig. 3, a matrix of normalized counts was constructed using all differentially expressed genes (padj < 0.05; LFC >2) from pairwise comparisons between conditions (n=2,660 genes) and k-means clustering of rows was performed (k=4).

Multivariate analysis of clinical data

For cross-validation of CLL-RNA sequencing analysis obtained (Fig. 3A-C, fig. S6A), we assessed the clinical impact of stromal PKC-β dependent gene expression through data generated from PBMCs derived from a cohort of fludarabine-resistant CLL patients (n=51) subsequently treated with subcutaneous Alemtuzumab in a multicenter phase 2 trial*(23)*, (NCT00274976). Patient sampling was performed at enrollment and prior to Alemtzumab treatment. Profiled mRNA was extracted using the Allprep DNA/RNA mini kit (Qiagen) on PBMCs purified using ficoll density gradient centrifugation. Quality control on purity, concentration and RNA integrity was assessed using the Agilent 2100 Bioanalyzer with the RNA 6000 Nano LabChip (Agilent Technologies) and the 2100 Expert Software. Samples used had an RNA Integrity Number (RIN) ≥ 7.0. Affymetrix GeneChip® Human Exon 1.0 ST Array (Affymetrix) were used for expression profiling. Per sample, 250 ng RNA were amplified, transcribed to cDNA, fragmented and subsequently labeled with biotin. Array hybridization was performed at 45°C for 16-18h in the Affymetrix GeneChip Hybridization Oven 640, arrays were subsequently washed in the Fluidics Station 450 and scanned with the GeneChip scanner 3000 7G. Experiments were conducted according to the manufacturer's protocol.

Raw Affymetrix Human Exon array (HuEx-1_0-st-v2) data files were preprocessed by the robust multichip average (RMA) algorithm using Aroma. Affymetrix gene expression values were summarized on the transcript level using the ‘core’ probe set definition according to Affymetrix. The Genesis platform*(64)* was used for clustering. Respective cluster and survival analysis was conducted only for genes impacting survival and showing co-expression. Hierarchical clustering was used with Manhattan distance and complete linkage. Clinical endpoints used for the survival analysis were progression-free survival (PFS) and overall survival (OS), data was missing in 2 patients.

Plasma membrane profiling

Plasma membrane profiling was performed as described previously *(65)*. Peptides were subsequently labelled with TMT reagents (Thermo Fisher Scientific), pooled and cleaned up using a SEP-PAK C18 cartridge (Waters) prior to high pH RP fractionation as previously described*(66)*. High pH fractions were pooled orthogonally into 12 samples for analysis by LC-MS on an Orbitrap Fusion (Thermo Fisher Scientific) utilising synchronous

precursor selection mode to isolate reporter ions essentially as previously described*(8)*. Data were searched using the MASCOT (Matrix Science, UK) search node within Proteome Discoverer v2.1 (Thermo Fisher Scientific). The database used was the SwissProt Mouse Reference Proteome including an appended database of common contaminants. Statistical differences between replicate groups were assessed using an implementation of LIMMA within the R environment including Benjamini-Hochberg correction for multiple hypothesis testing. The resulting p/q-values are reported. Experiment was performed in triplicate using one patient sample. For the heat-map shown in Fig. 5C, a matrix was constructed of the log2 transformed abundance values with the addition of a pseudo-count of 8 for all mid- to high-confidence protein measurements. This matrix was then used for k-means clustering (k=5) for each replicate across each condition. The side plot of the figure was generated using the median value of the abundance values for each replicate. The plot was generated using the seqsetvis R package (Boyd J (2018)) including Benjamini-Hochberg correction for multiple hypothesis testing.

Flow cytometry

All antibodies for flow cytometry measurements, as well as their respective isotype controls, were obtained either from BD Biosciences, Biolegend, eBioscience, Tonbo Biosciences, or Santa Cruz Biotechnology. For apoptosis analyses, FITC-Annexin V and DAPI (Biolegend) were used. A complete list of all antibodies used for this study can be found in the supplementary information (table S2).

CRISPR/Cas9-mediated gene deletions

Single-guide RNA (sgRNA) sequences were cloned into lentiCRISPRv2. Control_sgRNA (TCGGCACTGGCGATCGGTTG), Vcam1_sgRNA (GCTGGAACGAAGTATCCACG), Tfeb_sgRNA_1 (TGGACACGTACTGTCCACCT), Tfeb_sgRNA_2 (CTGTAGTTGAGAGAAGACGC), Tfeb_sgRNA_3 (TGAGATGCAGATGCCTAACA), Tfeb_sgRNA_4 (CCTCTGTGGATTACATCCGG). Lentiviral infections of murine bone marrow stromal cells with the specific sgRNA constructs were performed. Following 48 hours of puromycin selection (2 µg/ml), cells were negatively sorted for Vcam1 expression and cultured for further experiments, while *Tfeb*-deleted stroma were left unsorted after 72 hours of puromycin selection (2 µg/ml).

Neutralizing antibody assay

Bone marrow MSCs were seeded at a concentration of $1*10^4$ cells per well of a 96-well plate and incubated for 24 hours. Prior to addition of CLL cells 10mg/ml of neutralizing or control antibody, αVCAM1 and Control Rat IgG2a (both Biolegend), was added for 1 hour. CLL cells were then seeded at $2*10^5$ cells per well for monoculture and co-culture conditions. Neutralizing antibodies were restored to 10 mg/ml following the addition of CLL cells. After 24 hours venetoclax was administered at 2.5 nM and incubated for a further 48 hours before flow cytometric analysis.

Ibidi flow chamber cell adhesion assay

Stromal cells of respective genotype, *Prkcb*$^{+/+}$ and *Prkcb*$^{-/-}$, were seeded at a concentration of $3*10^4$ cells/100 μl into the channel of Ibidi channel tissue-culture treated μ-slides (Ibidi; type 1, 0.4 mm). 12 hours later fresh media was added simultaneously to both reservoirs. Primary CFSE-labeled CLL cells were counted by two individuals using trypan blue staining. The average of both counts determined the respective seeding cell numbers of each patient. After simultaneous removal of all reservoir media from channel slides, 500 μl of patient cell suspension was placed in one of the experiment-long designated influx reservoirs. Flow-through from atmospheric pressure into the efflux reservoir was reapplied to the designated influx reservoir 3 times for each slide. Final flow-through from efflux reservoirs were counted twice for each slide, averaged, and subtracted from respective seeding cell counts for each patient to obtain percent adhesion. Subsequently, 300 μl of media was placed into both reservoirs simultaneously and incubated for 24 hours. Cells were then exposed to respective treatments after simultaneously withdrawal of culture media, and simultaneous application of treatment media. 48 hours later, flow-through using 500 μl of fresh media placed into the designated influx reservoirs were performed 3 times using fresh media each flow-through. Pass-throughs from the efflux reservoirs were collected and
counted twice for cells, averaged and subtracted from each slide-specific number of adhered cells.

Generation of *Prkcb*$^{-/-}$ stroma expressing constitutively active TFEB (caTFEB)

Plasmids pCIP-caHuTFEB and empty vector pCIP (Plasmids #79013,79009; Addgene) were linearized using ScaI-HF restriction enzyme (New England Biolabs) (Young, NP 2016), and subsequently purified using a NucleoSpin Gel Purification Kit (Machery-Nagel). Transfections of a parental PKC-β KO stroma were performed, using 5.0 μg of each respective linearized plasmid prepared with Lipofectamine 2000 transfection reagent (ThermoFisher Scientific). 48 hours post-transfection, transfected cells and untransfected control were cultured in stromal media (MEM + 10% FBS +10% Horse Serum) containing 2 μg/ml of puromycin for 72 hours (ThermoFisher Scientific).

In vivo models for CLL homing and engraftment

For CLL homing experiments primary Eμ-TCL1 tumor cells were labelled with 5 μM Carboxyfluorescein-succinimidyl-ester (CFSE; Life Technologies) per manufacturer's protocol. Post-confirmation of labeling by flow cytometry, $40*10^6$ cells were injected intravenously, and $1*10^6$ cells injected intraperitoneally into age-matched mice of two genotypes. Peripheral blood was drawn by tail vein bleeding, and analyzed by flow cytometry following erythrocyte depletion.

In vivo model for Vcam1 biomarker ± enzastaurin

Leukemic Eμ-TCL1 mice were analyzed for leukemic burden by $CD5^+C19^+$ staining of peripheral blood. Cohorts were assembled to match overall leukemic burden of vehicle control between enzastaurin treatment cohorts. Enzastaurin or vehicle (5% dextrose + 10% ethanol in water), was administered at a dose of 60mg/kg BID for a total of 96 hours. Analyses of bone marrow Vcam1 expression was conducted 3 hours following last treatment, by flow cytometry. In brief, stromal cell populations were isolated from femur and tibia, crushed in mortar and pestle, and digested with 2 ml of collagenase I (Stem Cell Technologies) and 1 mg/ml collagenase IV (Sigma-Aldrich,) at 37°C in strong agitation for 30 minutes. Cells were washed with PBS + 2% FBS and filtered through a 40 μm mesh filter. Red blood cells were lysed with Pharmalyse (BD Biosciences) for 10 minutes on ice. Aliquots from individual mice were analysed by flow cytometry (representative gating depicted in fig. S11C).

In vivo model for Lamp-1 and Lamp-2 biomarkers ± enzastaurin

72 hours post-transplantation TCL1-transplanted PKC-β WT recipients were treated with either vehicle, venetoclax (100 mg/kg per day), or pre-treated with enzastaurin (60 mg/kg BID) and concomitantly administered with enzastaurin + venetoclax for the duration of 3 days. Bone marrow was harvested 3 hours after administration of final dosing and subsequently analyzed for respective intracellular Lamp-1 and Lamp-2 expression after surface staining and subsequent fixation and permeabilization (Biolegend). Mean fluorescence intensities (MFIs) of Lamp-1 and Lamp-2 were assessed in viable MSCs ($CD45^{-}Ter119^{-}$) and non-MSCs ($CD45^{+}Ter119^{+}$). Statistical significance of intracellular staining was determined using an unpaired two-tail Student T-test.

In vivo CLL study of venetoclax ± enzastaurin

C57B/6J mice (Jackson Labs) were injected intraperitoneally with either $3.5*10^6$ or $5*10^6$ cells of two respective primary Eμ-TCL1 tumors. 72 hours post-transplantation respective treatments began by oral gavage for 16 consecutive days. Venetoclax was solubilized as previously reported *(67)*. In brief, venetoclax was formulated in phosal-50 propylene glycol (60%), polyethyleneglycol-400 (30%), and ethanol (10%). Leukemic burden was assessed by erythrocyte-depleted peripheral blood analyzed by flow cytometry.

In vivo CLL study of fludarabine ± enzastaurin

C57B/6J (Jackson Labs, UK) mice were injected intraperitoneally with $5*10^6$ cells of two respective primary Eμ-TCL1 tumors. 72 hours post-transplantation mice respective treatments began by oral gavage and intraperitoneal injection. Fludarabine phosphate (Sigma-Aldrich) was solubilized in sterile PBS. Mice received Fludarabine treatment for 5 consecutive days for two cycles. Enzastaurin or vehicle was administered twice daily of the same periods. Leukemic burden was assessed by peripheral blood analyzed by flow cytometry.

In vivo ALL-PDX study of vincristine ± enzastaurin

NOD.*Cg-Prkdc*^{scid}*Il2rg*^{tm1Wjl}/SzJ (NSG) mice were injected intravenously with $2\text{-}3*10^5$ cells of luciferase-transduced ALL xenografts cells derived from 2 unique patient samples. In 3

independent experiments, cohorts were respectively treated 72 hours post-transplantation. enzastaurin (60mg/kg BID) or vehicle control was administered orally, 12 hours prior to intraperitoneal dosing of vincristine or vehicle and continued for 72 hours thereafter. Vincristine (Sigma-Aldrich) was solubilized in sterile PBS and administered once per treatment cycle at a weight-adjusted dose between 0.5 mg/kg and 0.6 mg/kg *(68)*. Animals received equal treatment dosages between treated cohorts for each independent experiment, for one or two cycles. For the combination treated cohorts, 14 mice received one-cycle, whereas 5 mice received a second treatment cycle 4 weeks following initial treatment. Anesthesia-related morbidities on Day 73 post-transplantation in one independent experiment resulted in the censoring of 3 (vincristine) and 4 (combination treatment) animals. Leukemic burden was assessed by peripheral blood, which was analyzed by flow cytometry and by bioluminescent imaging (Xenogen IVIS). Luciferin was administered intraperitoneally to anesthetized animals prior to live imaging.

Statistical analysis

Statistical analyses of results were performed using one-way ANOVA followed by two-tail Student t-tests, with respective unpaired and paired analyses experimentally dependent. Statistical annotations as previously noted were denoted with asterisks according to the following, **** $p < 0.0001$, *** $p < 0.001$, ** $p < 0.01$, * $p < 0.05$, and ^{ns} $p > 0.05$.

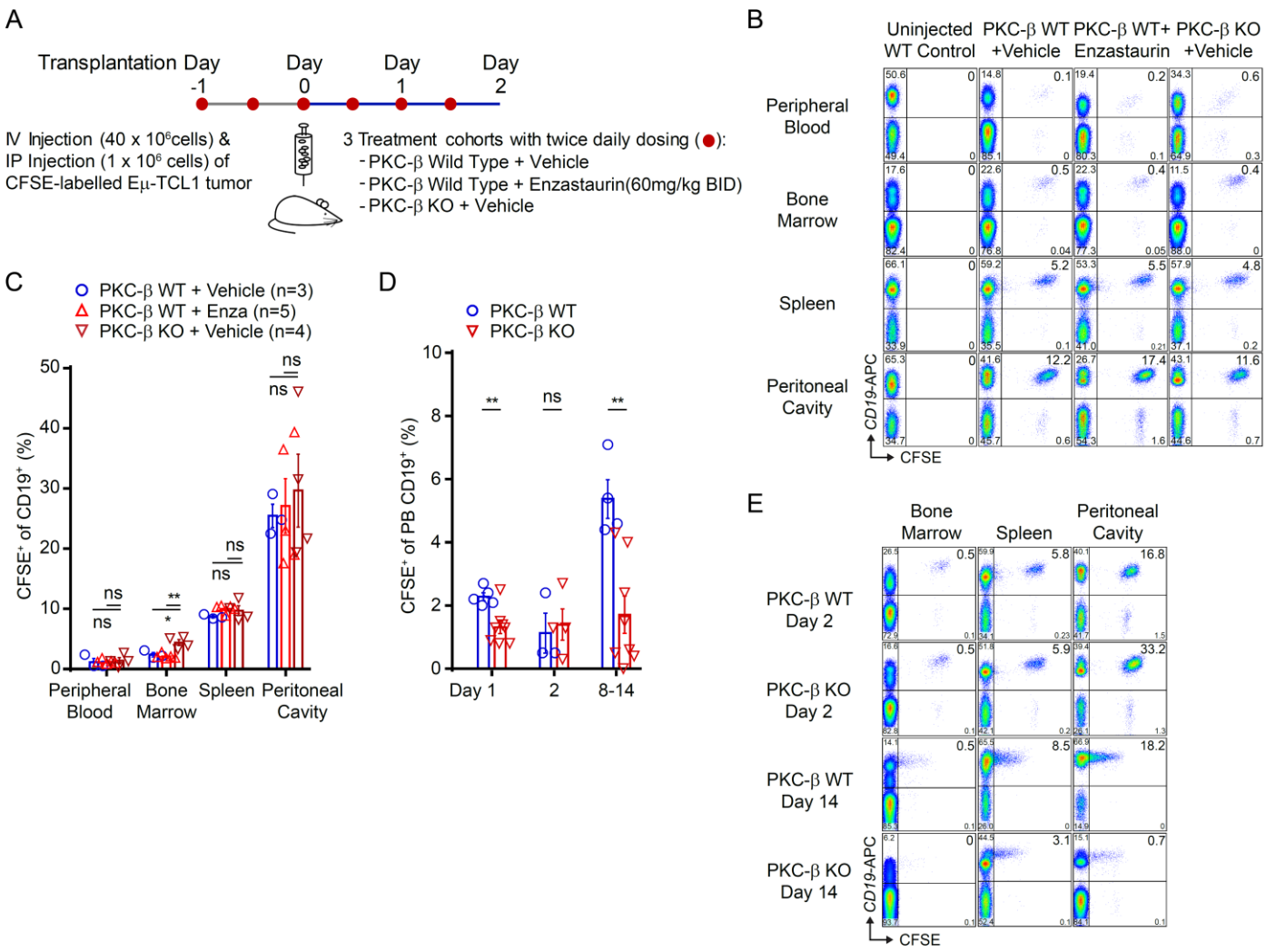

Fig. S1. Homing and engraftment kinetics of Eμ-TCL1 tumor cells in PKC-β wild-type and null mice. (A) An experimental scheme to assess homing of Eμ-TCL1 cells in PKC-β WT and KO mice, respectively. **(B)** Representative $CD19^+$ FACS plots of four tissue compartments, 48 hours post-transplantation of CFSE-labeled Eμ-TCL1 cells. **(C)** Homing of CFSE-labelled Eμ-TCL1 cells was quantified as a percentage of total $CD19^+$ cells ±SEM. **(D)** Quantification of CFSE-labelled Eμ-TCL1 cells as a percentage total $CD19^+$ cells detected in the peripheral blood at indicated time-points (Day1: WT, n=5; KO, n=8; Day 2: WT, n=3; KO, n=4; Days 8-14: WT, n=6; KO, n=8). Analyses are pooled from independent experiments using two primary tumors. **(E)** Representative FACS plots of bone marrow, spleen, and peritoneal cavity on day 2 and day 14 post-transplantation of CFSE-labeled Eμ-TCL1 cells, respectively.

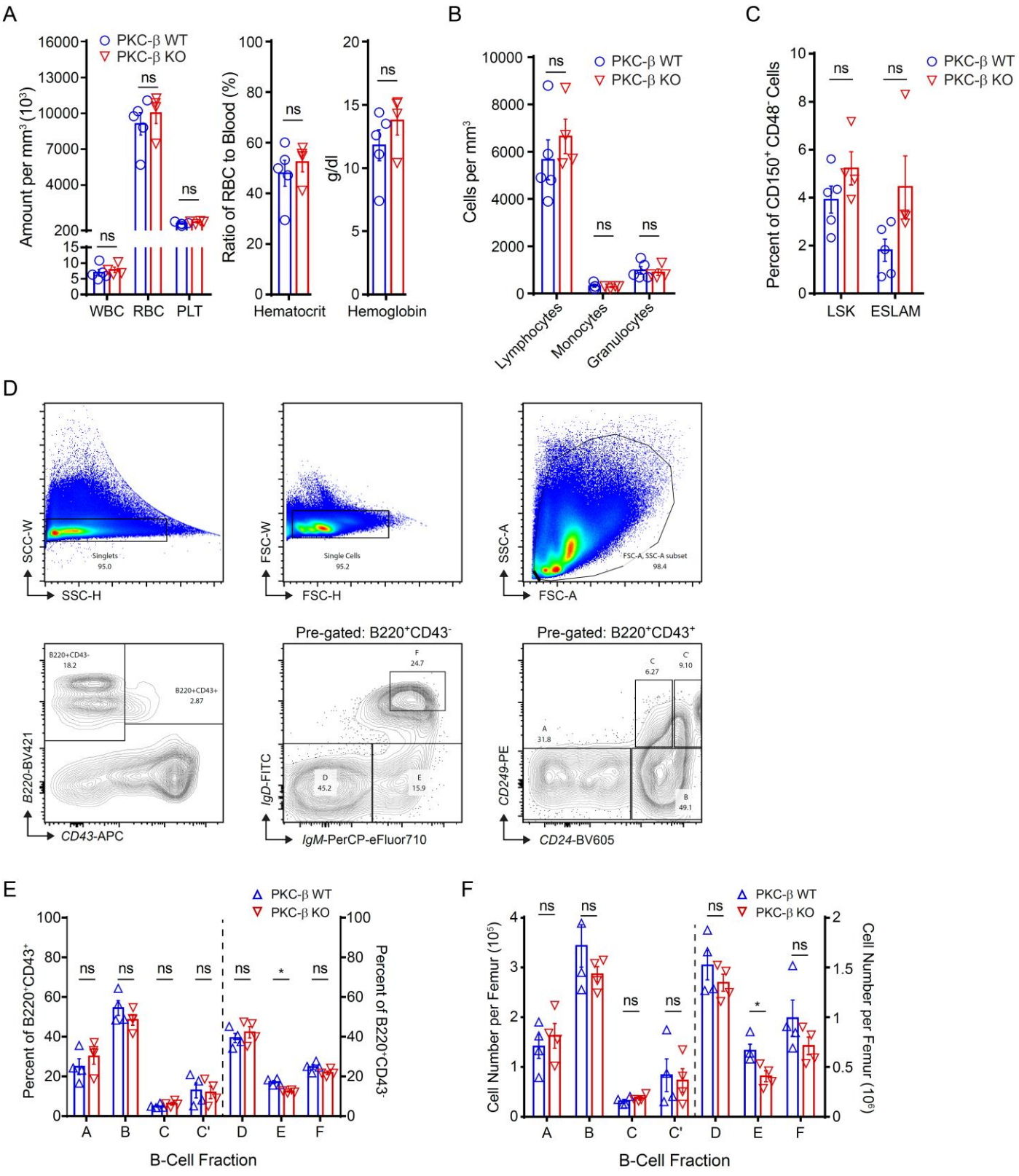

Fig. S2. PKC-β deficiency does not overtly alter hematopoiesis. (A) White blood cell (WBC), red blood cell (RBC), and platelet (PLT) abundance are shown from complete blood counts of peripheral blood from age-matched PKC-β WT and KO mice. **(B)** Individual abundance of white blood cell types is graphically shown. **(C)** Bone marrow composition of $Lin^{-}Sca1^{+}C\text{-}Kit^{+}$ (LSK) and $CD150^{+}CD48^{-}CD45^{+}EPCR^{+}$ (ESLAM) hematopoietic stem cells are shown as a percentage of $CD150^{+}CD48^{-}$ cells. **(D)** Representative gating strategy of bone marrow B-cell progenitors. **(E)** Composition of B-cell

progenitor fractions (Hardy fractions) are shown as a percentage of $B220^{+}CD43^{+}$ (left axis, Fraction A-C') and of $B220^{+}CD43^{-}$ (right axis, Fraction D-F). **(F)** Absolute numbers of B-cell progenitor fractions (Hardy fractions) are shown as a total of RBC-lysed bone marrow from a respective femur of PKC-β WT (n=4) and KO (n=4) mice (left axis, Fractions A-C'; right axis, Fraction D-F).

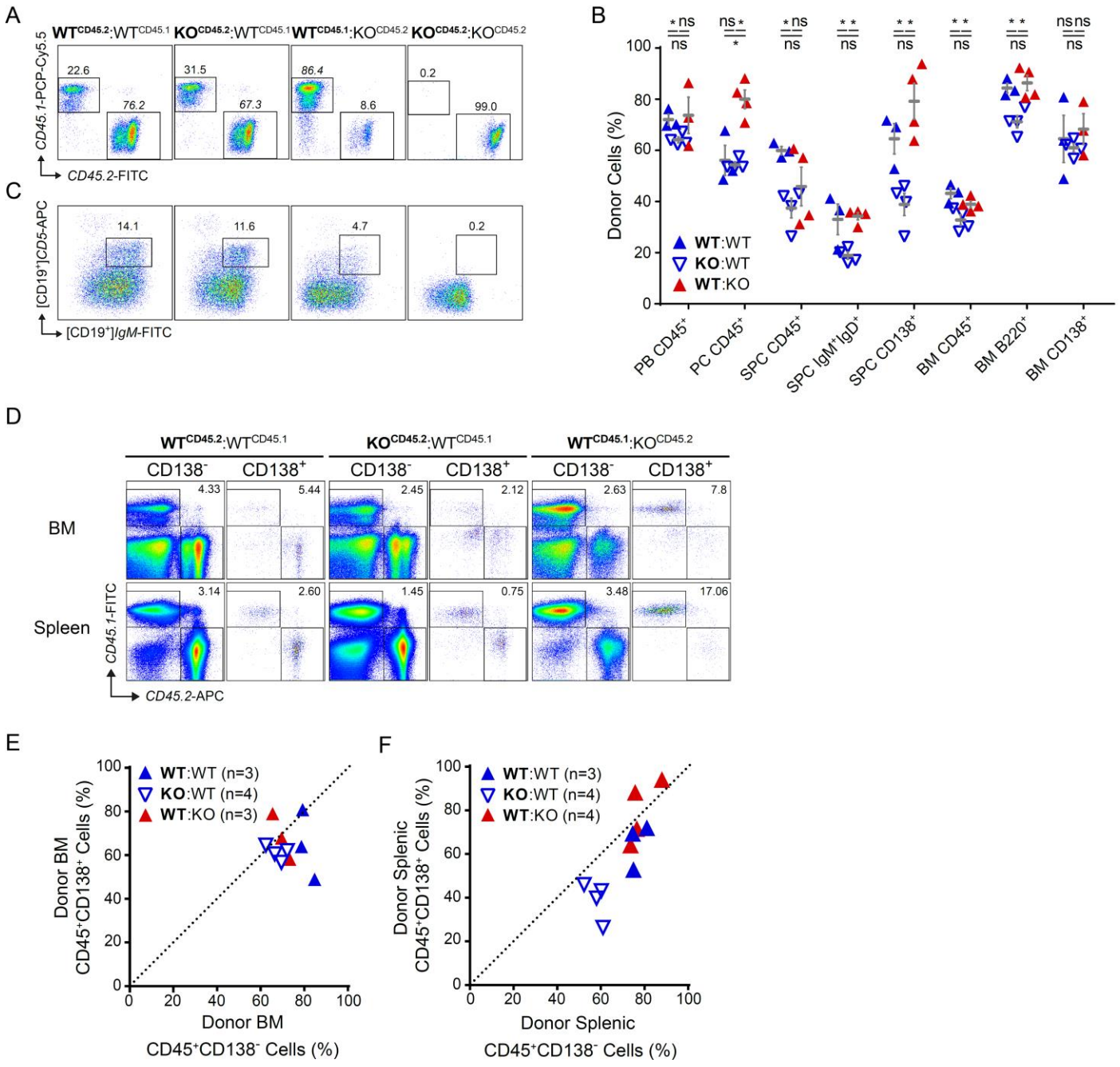

Fig. S3. PKC-β chimeras engraft with comparable efficiency irrespective of donor or recipient genotype. (A) Representative CD45.1 and CD45.2 FACS plot stains of peripheral blood, 8 weeks post-transplantation, are shown with the donor label and percentage of donor cells denoted in bold. **(B)** Representative CD5 and IgM FACS plots for $CD19^+$ cells of the peritoneal cavity are shown for the similarly labeled cohorts as above in fig. S3A. **(C)** Assessment of chimerism in mice with mismatched CD45 isotypes. Percentages of respective donor CD45 isotype are shown ±SEM. Genotype of donor BM is set in bold; **WT**:WT (n=3), **KO**:WT (n=4), and **WT**:KO (n=4; n=3 for PB $CD45^+$ and BM $CD138^+$). Abbreviations for tissues as follows: PB, peripheral blood; PC, peritoneal cavity; SPC, splenocytes; BM, bone marrow. Ten weeks post transplantation, a mixed chimerism was observed in the peripheral blood with a predominance of the transplanted bone marrow cells (**WT**(donor):WT(recipient)=72.0% ±2.09%, **WT**:KO=73.7 ±7.11%, **KO**:WT=64.1% ±1.13%. **(D)** Representative $CD45.1^+$ and $CD45.2^+$ stains of respective $CD138^-$ and $CD138^+$ BM or splenic cells are shown. Ratios of donor : recipient are indicated within respective stains. **(E)** Graphs of percent donor BM $CD45^+CD138^-$ cells and percent donor BM $CD45^+CD138^+$ cells are plotted, with equal donor engraftment of both ±CD138 compartments depicted by the dotted line. Percentages of donor cells are shown as a subset of total $CD45^+$ cells. **(F)** Graphs of splenic donor $CD45^+CD138^-$ engraftment and splenic donor $CD45^+CD138^+$ engraftment are plotted. Percentages of donor cells reflect the percent of total $CD45^+$ cells.

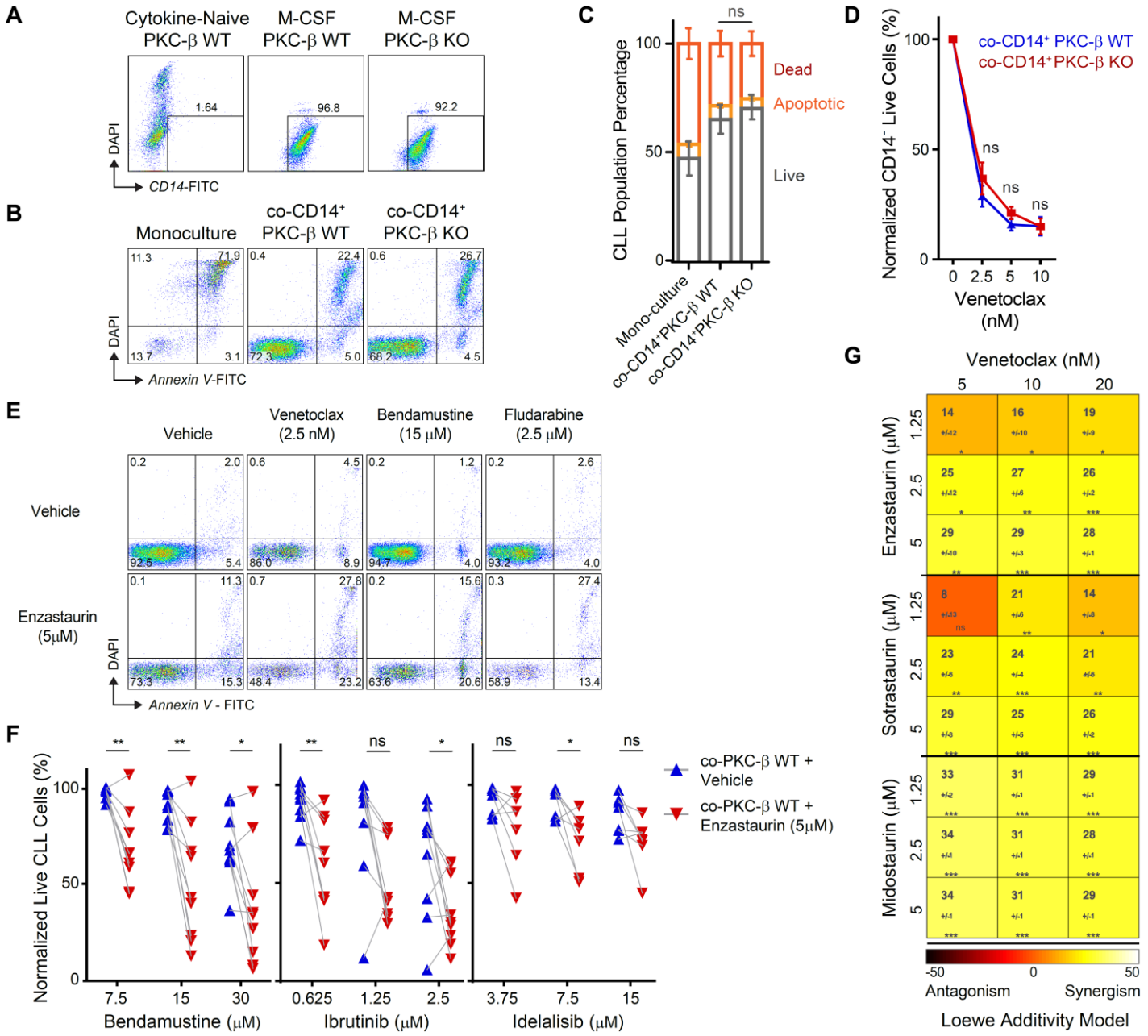

Fig. S4. Monocytes confer CLL survival support but not PKC-β dependent EMDR, in contrast to MSCs. (A) Representative flow cytometry plots of cytokine-naive PKC-β WT, and M-CSF cultured PKC-β WT and PKC-β KO stroma. **(B)** Representative Annexin-V and DAPI flow cytometry plots of mono-cultured or respective co-cultured CLL cells, 72 hours post-seeding of CLL. **(C)** Percentage of Live (Annexin-V$^-$, DAPI$^+$), Annexin-V$^+$, and Dead (DAPI$^+$Annexin-V$^{+or\ -}$) stained cells are shown for individually co-cultured primary CLL (n=5 unique patients) for the three respective conditions. Statistical comparisons are shown for the live-cell fractions of each condition. **(D)** Viability of CLL cells following 72 hours of respective co-culture (CD14$^+$ PKC-β WT or CD14$^+$ PKC-β KO cells) with 48 hours of exposure to increasing doses of venetoclax (n=6). **(E)** Representative Annexin-V and DAPI flow cytometry plots of mono-cultured or respective co-cultured CLL cells, 72 hours post-seeding of CLL. **(F)** Viability of CLL cells following 72 hours of PKC-β WT co-culture with 48 hours of exposure to increasing doses of respective bendamustine (n=8), ibrutinib (n=9), or idelalisib (n=7) ± enzastaurin treatment. Statistical significance was assessed using a paired two-tail Student-T-test. **(G)** Synergism was calculated using Combenefit Software (CRUK), within the Loewe additivity model, for venetoclax combined with enzastaurin, sotrastaurin, or midostaurin, respectively (n=6 per combination).

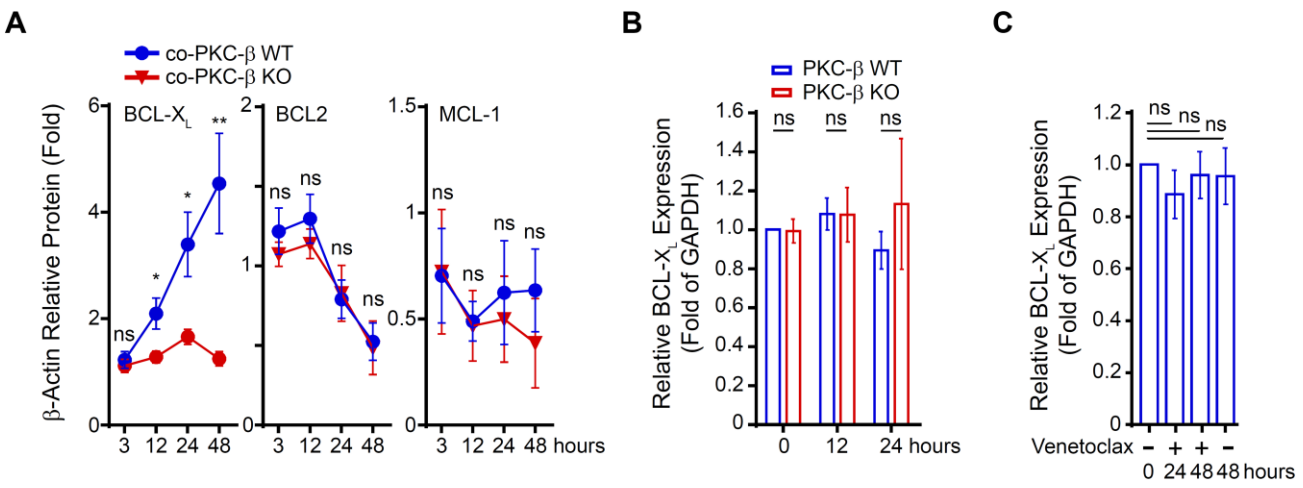

Fig. S5. PKC-β-mediated EMDR involves increased protein levels of BCL-X_L. (A) Graphs of respective BCL-X_L (n=5), BCL-2 (n=5), MCL-1 (n=3) fold protein levels in CLL cells co-cultured with either PKC-β WT or PKC-β KO, relative to β-Actin after indicated exposures to 2.5 nM venetoclax. **(B)** Quantitative-PCR measured relative BCL-X_L expression in CLL (n=4) in the respective presence of PKC-β WT or KO stromal co-culture ($2^{-\Delta\Delta CT}$). **(C)** Quantitative-PCR measured relative BCL-X_L expression in CLL (n=6) co-cultured with PKC-β WT ± venetoclax treatment (2.5 nM) for the indicated timepoints.

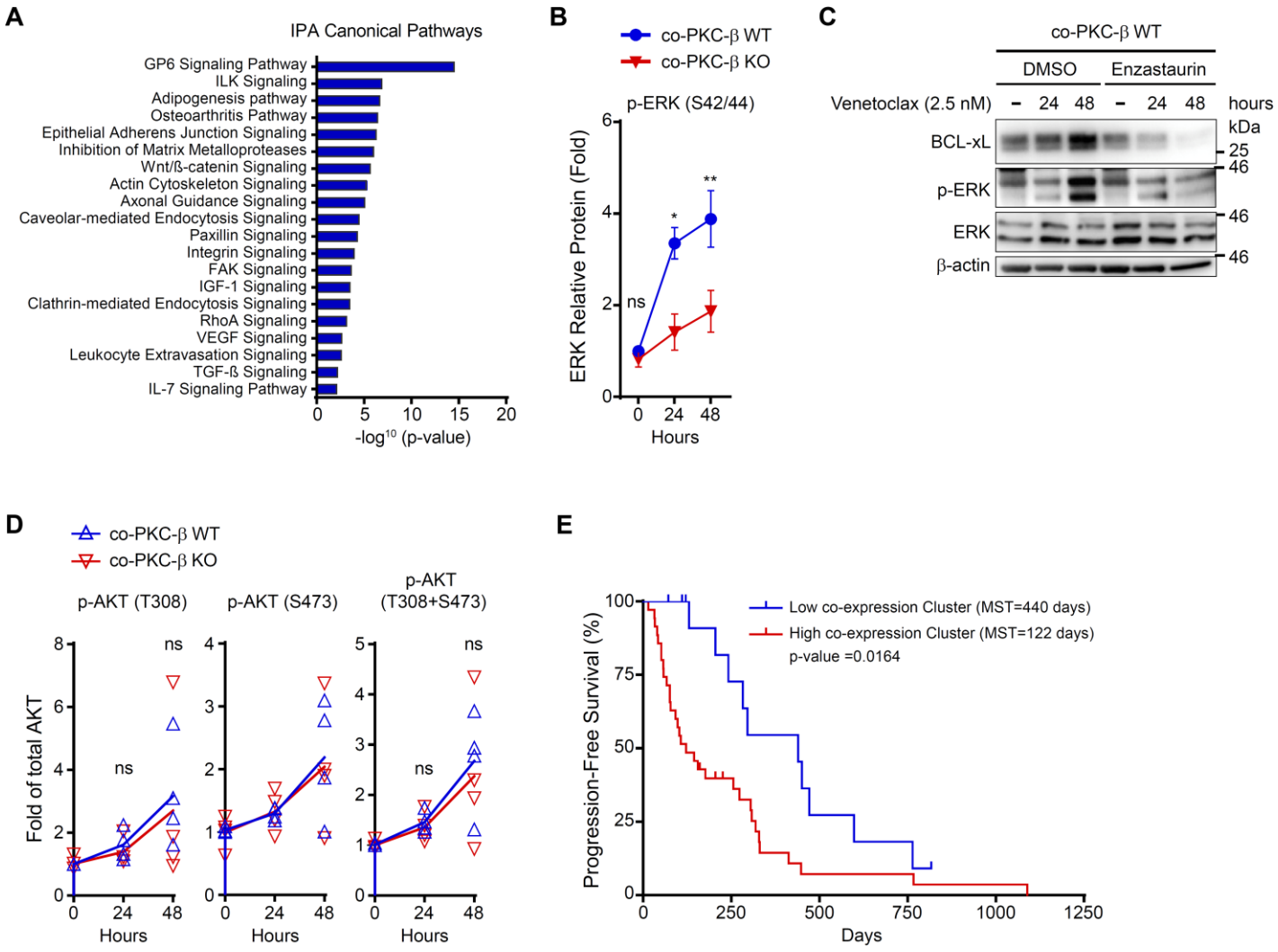

Fig. S6. CLL signaling pathways regulated by stromal PKC-β correlate with clinical outcomes. (A) IPA analysis of canonical pathways activated in CLL cells (n=3) co-cultured with PKC-β WT stroma compared to CLL cells co-cultured with PKC-β KO stroma (n=3), both in the presence of venetoclax (1.25 nM). **(B)** Graph of p-ERK (n=4) fold protein levels in CLL cells co-cultured with either PKC-β WT or PKC-β KO, relative to total ERK after indicated exposures to 2.5 nM venetoclax. **(C)** BCL-X_L, phosphorylated ERK (Thr202/Thr204), total ERK and β-actin immunoblots of primary CLL at indicated time-points of venetoclax treatment, co-cultured with PKC-β WT stroma ± enzastaurin (5 μM). **(D, related to Fig. 3I)** Graphs of respective phosphorylated-AKT relative fold protein levels in CLL cells co-cultured with either PKC-β WT or PKC-β KO after indicated exposures to 2.5 nM venetoclax. **(E, related to Fig. 3K)** Kaplan-Meier curves (x-axis with time since treatment) according to respective clusters (”High co-expression” vs. “Low co-expression”), showing statistically significant differences (pairwise log-rank tests) for median progression-free survival (PFS) (”High co-expression”: 122 days vs “Low co-expression”: 440 days; p<0.02).

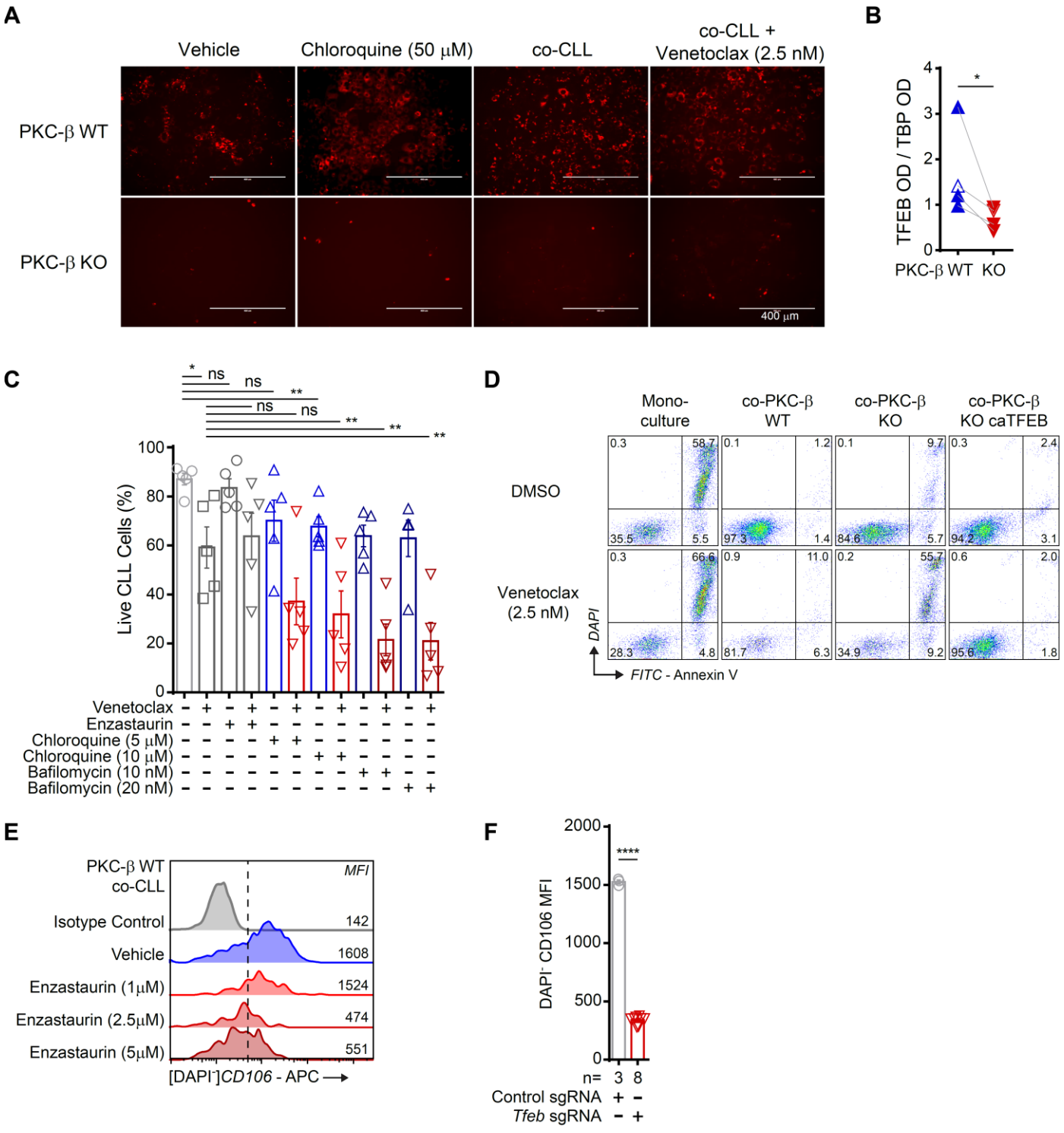

Fig. S7. Stromal lysosomes, and lysosomal biogenesis regulator TFEB, are central to PKC-β-mediated EMDR. (A) Lysosomal staining using Lysotracker Red (50 nM for 30 mins) of passage-matched naive PKC-β WT stroma and PKC-β KO stroma, respectively ± chloroquine (50 mM for 1hr), and co-cultured stroma of both PKC-β genotypes ±venetoclax (2.5 nM). **(B, related to Fig. 4E)** Analysis of stromal optical density of nuclear TFEB/TBP ratios for indicated PKC-β WT and KO stroma (CLL co-cultures denoted by solid symbols and naive stroma denoted by open symbols). Statistical significance assessed using two-tailed ratio-paired t-test. **(C)** CLL viability assay (n=5) co-cultured on stroma 12 hours after pre-treatment with enzastaurin, chloroquine, or bafilomycin for 6 hours followed by washout prior to CLL-seeding. Venetoclax treatment was applied in noted conditions 24 hours post CLL-seeding. **(D)** Representative FACS plots of CLL cells from mono-cultured or respective co-cultured CLL cells, 72 hours post-seeding and 48 hours post-treatment of CLL.

(E) *In vitro* downregulation of Vcam1 in PKC-β WT stroma co-cultured with CLL ±increasing concentrations of enzastaurin. **(F, related to Fig. 5H)** Graph of CD106 (Vcam1) MFIs from mono-cultured PKC-β WT stroma with Crispr-deleted cells transduced with sgRNA control (n=3) or *Tfeb*-deleted stroma using 4 unique sgRNAs, respectively (n=8 total values; duplicate measurements for n=4 sgRNAs).

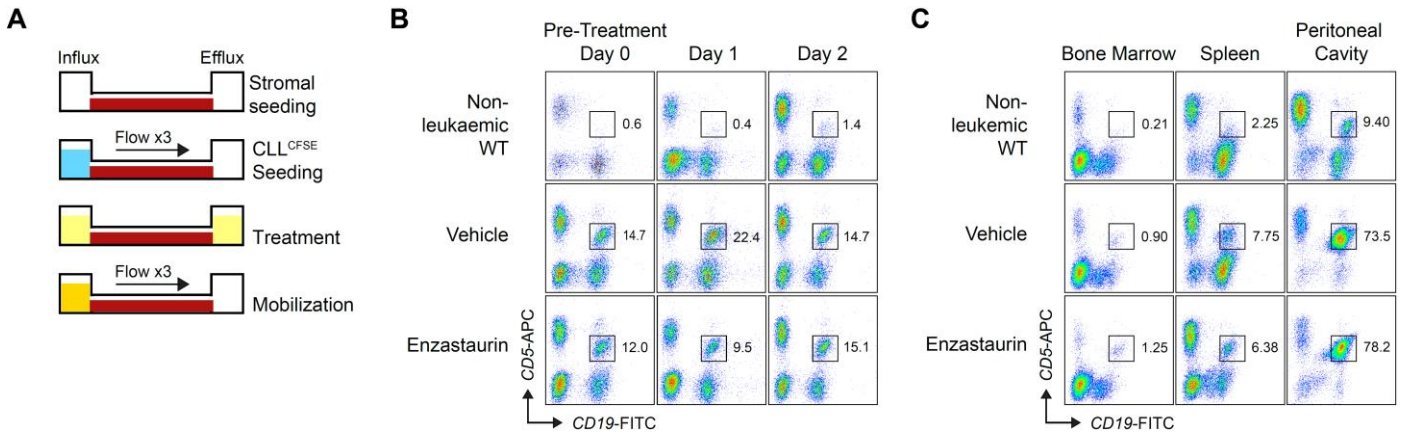

Fig. S8. PKC-β is dispensable for *in vitro* and *in vivo* mobilization of leukemia. (A) Schematic of adhesion and mobilization assays utilizing channel slides. **(B, related to Fig. 5K)** Representative flow cytometry plots of $CD19^{+}CD5^{+}$ cells in the peripheral blood before and during treatment with enzastaurin or vehicle, respectively. **(C, related to Fig. 5L)** Representative flow cytometry plots of $CD19^{+}CD5^{+}$ cells in the bone marrow, spleen, and peritoneal cavity after treatment with enzastaurin or vehicle, respectively.

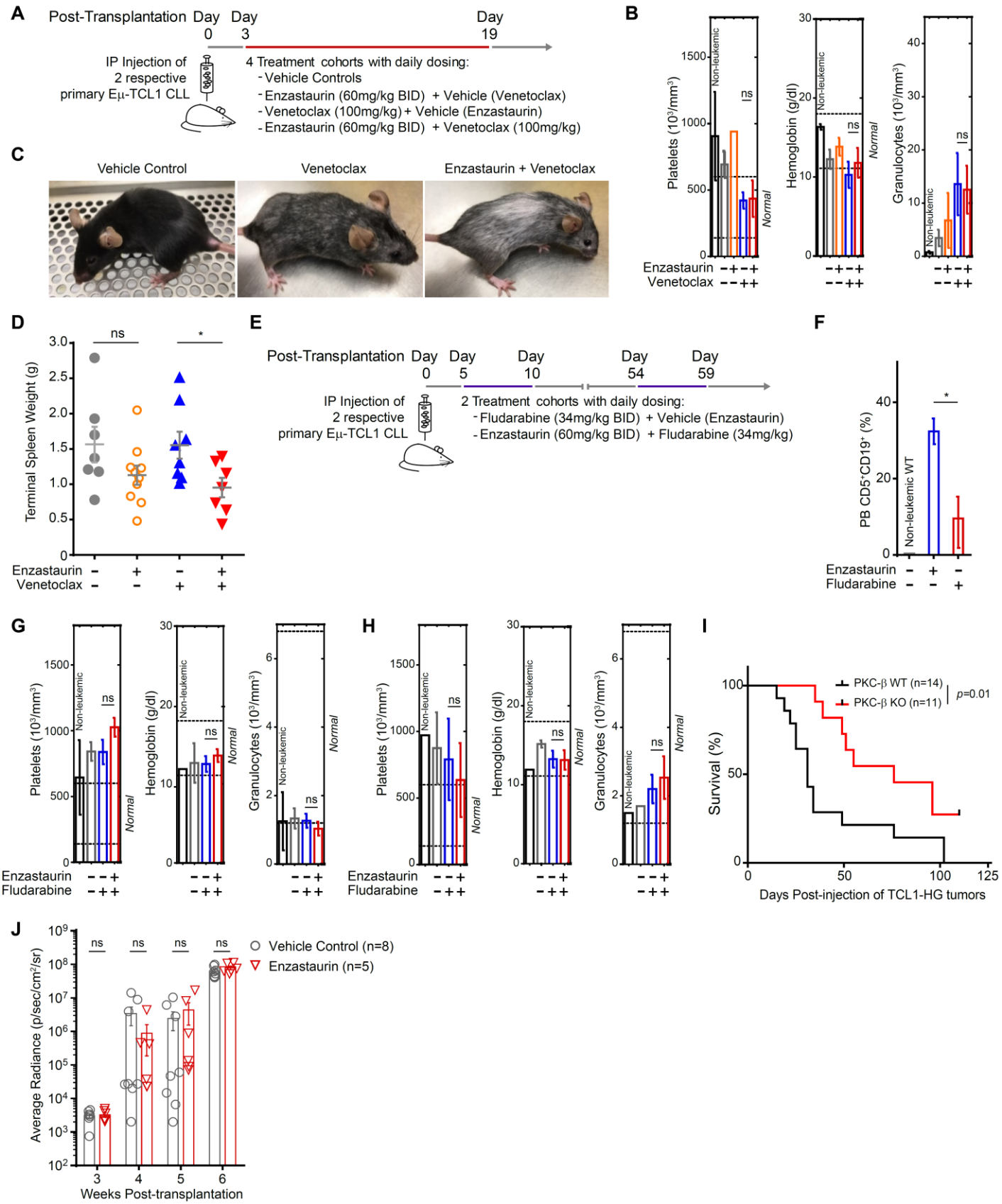

Fig. S9. *In vivo* co-targeting of PKC-β does not contribute to increased off-target cytotoxicity. (A) *In vivo* treatment schematic of Eμ-TCL1 CLL model using venetoclax, enzastaurin, mock control or venetoclax + enzastaurin. **(B)**

Complete blood counts (CBC) of non-leukemic WT control (n=2), vehicle control (n=4), enzastaurin-treated (n=4), venetoclax-treated (n=4), and enzastaurin + venetoclax treated (n=4) mice on Day 32 post-end of treatment. Normal blood counts are indicated between dashed lines. Statistical differences were calculated by unpaired Student T-Test. **(C)** Photographs at week 12 post-treatment of representative mice from vehicle, venetoclax, and enzastaurin + venetoclax treatment cohorts. **(D)** Terminal spleen weights for individuals of indicated treatment cohorts. **(E)** Schematic of *in vivo* treatment model of Eμ-TCL1 CLL using fludarabine + vehicle or fludarabine + enzastaurin. **(F)** Percentage of detectable peripheral blood $CD5^{+}CD19^{+}$ cells in non-leukemic controls (n=3), fludarabine-treated (n=3) and fludarabine + enzastaurin treated mice (n=4), on days 25 - 28 post-end of first treatment cycle. **(G)** Complete blood counts of non-leukemic WT control (n=2), vehicle control (n=3), fludarabine-treated (n=3), and enzastaurin + fludarabine treated (n=3) mice on Day 16 post-end of first-treatment cycle. **(H)** Complete blood counts of non-leukemic WT control (n=1), vehicle control (n=2), fludarabine-treated (n=3), and enzastaurin + fludarabine-treated (n=3) mice on Day 10 post-end of second-treatment cycle. **(I)** TCL1-HG cells were transplanted into either PKC-β WT (MST= 31 days) or PKC-β KO recipients (MST= 76 days). **(J)** Average radiance obtained by bioluminescent imaging of ALL-PDX engrafted NSG animals treated with either vehicle control or enzastaurin. Statistical significance was determined using an unpaired two-tail Student T-test.

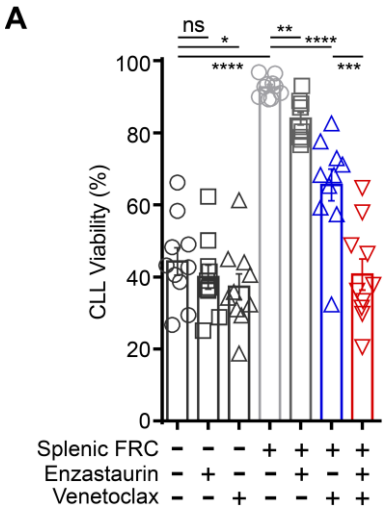

Fig. S10. EMDR derived from splenic stroma is mitigated by PKC-β antagonism. (A) *In vitro* treatment of primary CLL (n=10) in monoculture or co-culture on splenic FRC stroma ($gp38^{+}CD31^{-}$) treated with either vehicle control, enzastaurin, venetoclax, or venetoclax + enzastaurin. Statistical significance was determined using a paired two-tail Student T-test.

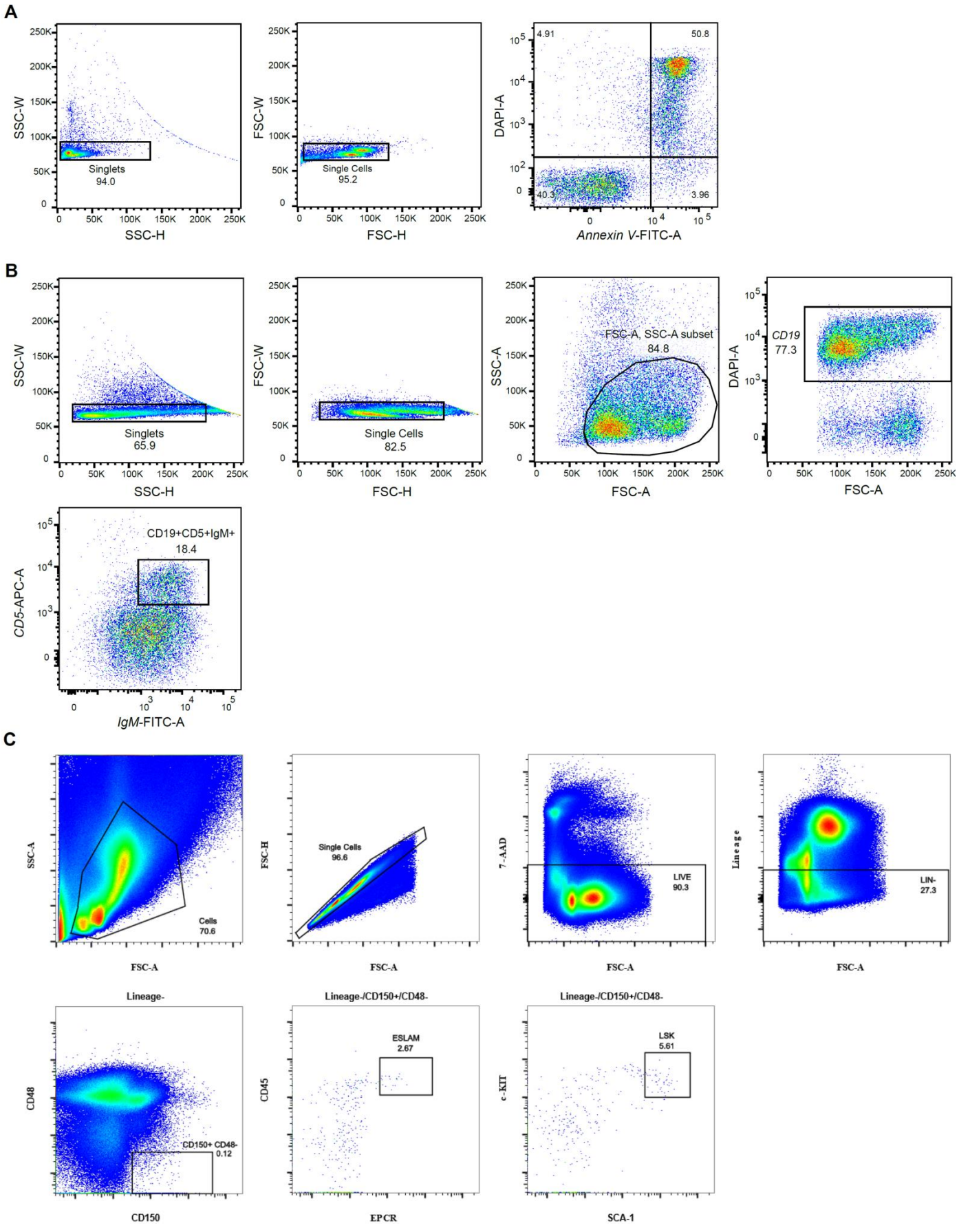
A
SSC-W
SSC-H
Singlets
94.0
FSC-W
FSC-H
Single Cells
95.2
DAPI-A
Annexin V-FITC-A
4.91
50.8
40.3
3.96
B
SSC-W
SSC-H
Singlets
65.9
FSC-W
FSC-H
Single Cells
82.5
SSC-A
FSC-A
FSC-A, SSC-A subset
84.8
DAPI-A
CD19
77.3
FSC-A
CD5-APC-A
IgM-FITC-A
CD19+CD5+IgM+
18.4
C
SSC-A
FSC-A
Cells
70.6
FSC-H
FSC-A
Single Cells
96.6
7-AAD
FSC-A
LIVE
90.3
Lineage
FSC-A
LIN-
27.3
Lineage-
CD48
CD150
CD150+ CD48-
0.12
Lineage-/CD150+/CD48-
CD45
EPCR
ESLAM
2.67
Lineage-/CD150+/CD48-
c-KIT
SCA-1
LSK
5.61

Fig. S11. Representative FACS gating strategies. (A) Representative FACS gating for co-culture in vitro cytotoxicity assays (left to right). **(B)** FACS gating strategy for immunophenotyping of peritoneal cells from chimeric mice (left to right, per row). **(C)** Representative FACS gating strategy for in vivo HSC phenotyping (left to right, per row).

Supplemental Table S1: Patient characteristics

Chronic lymphocytic leukemia (Figures 2-5,S4-S7,S9-S11)			
Encrypted Patient ID	**Cytogenetic results/ IGVH-status***	**Live cell decrease w/enzastaurin + venetoclax (5 nM) vs. venetoclax alone**	**Live cell decrease w/enzastaurin +fludarabine (2.5 uM) vs. fludarabine alone**
BP0401	Del13q14, M-IGVH	57.9%	40.8%
BS4072	Del13q14, UM-IGVH	-0.8%	37.9%
CL9959	Data not available	45.8%	28.5%
DP3335	Del13q14, M-IGVH	48.4%	19.2%
KA9559	Negative FISH panel	26.4%	14.2%
DI7353	Del13q	55.7%	-1.9%
BF59	Del13q, Del17p	51.3%	-3.7%
JC2614	Normal FISH panel, UM-IGVH	69.4%	5.8%
SJ35	Data not available	80.8%	25.1%
MB6377	Del17p	23.8%	24.4%
MO2147	P53 mutated	41.9%	56.5%
EB5492	Trisomy12	14.7%	2.3%
CH8051	Del17p	33.4%	-1.9%
EG5792	Trisomy12	25.6%	18.9%
AR30	Del13q, Del11q	27.4%	16.8%
AS5041	Del13q, Del17p, Del11q	40.4%	-3.1%
JC833	Del13q, Del11p	16.7%	21.8%
SM7753	Del13q, Del17p, Trisomy12	27.2%	-3.8%
PF8841	Del17p, Trisomy13q14	37.5%	37.0%
DW5916	Trisomy 12	19.1%	13.0%
Mantle Cell Lymphoma (Figure 6F)			
Encrypted Patient ID	**Cytogenetic results/ IHC/FC**	**Live cell decrease w/enzastaurin + venetoclax (2.5 nM) vs. venetoclax alone**	**Live cell decrease w/enzastuarin + venetoclax (5 nM) vs. venetoclax alone**
12414	t(11;14), Cyclin D1+	19.6%	25.8%
10084	t(11;14), Cyclin D1+	40.4%	34.0%
12267	t(11;14), Cyclin D1+	40.9%	46.8%
FC0175	$CD19^+$, $CD20^+$, $CD79b^+$ $CD5^+$, $CD200^-$ (FISH unavailable)	43.9%	41.7%
PG220	Data not available	47.1%	38.9%
V314	Blastoid MCL, Cyclin D1+	3.8%	1.8%
V323	t(11;14), monosomy 12 Cyclin D1+, p53 Del	39.2%	27.1%
M13	CD5+, PAX5+, FCM7++	9.5%	6.8%
B-Acute lymphoblastic leukemia (Figure 6G,H)			
Encrypted Patient ID	**Cytogenetic results**	**Live cell decrease w/enzastaurin + dexamethasone (0.1 nM) vs. dexamethasone alone**	**Live cell decrease w/enzastaurin + vincristine (50 nM) vs. vincristine alone**
190615A	Complex Karyotype	81.4%	57.8%
310315A	MLL-AF9	-	47.1%
201115A	TEL-AML1	15.3%	39.7%
260416A	TEL-AML1	76.3%	33.5%
261215A	TEL-AML1	70.0%	42.6%
170815A	E2A-PBX1	41.3%	34.9%
080915A	Hyperdyploid	18.4%	13.3%
130516A	TEL-AML1	15.0%	43.3%
131015A	High-Hyperdyploid	56.6%	13.3%
170816A	High-Hyperdyploid	21.1%	11.4%

* UM/MIGVH=unmutated/ mutated IGVH
IHC=immunohistochemistry
FC=flow cytometry

Supplemental Table S2: Key resources

Antibodies	Source	Catalog #
Anti-Human FcR (1:200 dilution)	Biolegend	422302
Anti- Mouse FcR (1:200 dilution)	Biolegend	101320
Anti-Mouse CD45.1 (A20)–FITC (1:200 dilution)	Tonbo Bioscience	35-0453-U500
Anti-Mouse CD45.2 (104)–APC (1:200 dilution)	Biolegend	109814
Anti-Mouse CD45.1 - PerCP/Cy5.5 (1:200 dilution)	Biolegend	110728
Anti-Human CD19 - APC (1:200 dilution)	Biolegend	302212
Anti-IgM-FITC (1:200 dilution)	Biolegend	406506
Anti-Mouse CD138-BV421 (1:200 dilution)	Biolegend	142523
Anti-Mouse CD19-BV421 (1:200 dilution)	Biolegend	302233
Anti-Mouse CD5-APC (1:200 dilution)	Biolegend	100626
Anti-Mouse CD19-FITC (1:200 dilution)	Biolegend	101505
Anti-Mouse CD19-APC (1:200 dilution)	Biolegend	115112
Anti-Mouse CD106-APC (1:200 dilution)	Biolegend	105717
Anti-Mouse B220-BV421 (RA3-6B2) (1:100 dilution)	Biolegend	103239
Anti-Mouse CD24-BV605 (MI/69) (1:100 dilution)	Biolegend	101827
Anti-Mouse IgD-FITC (11-26c.2a) (1:100 dilution)	Biolegend	405704
Anti-Mouse CD43-APC (S7) (1:100 dilution)	Becton Dickinson Biosciences	560663
Anti-Mouse CD249-PE(6C3) (1:100 dilution)	eBioscience	12-5891-81
Anti-Mouse IgM-PerCPe710 (II/41) (1:100 dilution)	eBioscience	46-5790-82
Anti-Mouse Ter119-PeCy7 (1:200 dilution)	Becton Dickinson Biosciences	557853
Anti-Mouse CD45-PeCy7 (1:400 dilution)	eBioscience	25-0451-82
Anti-Mouse CD31-APC (1:100 dilution)	Becton Dickinson Biosciences	551262
Anti-Mouse CD51-BV (1:100 dilution)	Becton Dickinson Biosciences	740062
Anti-Mouse Sca-1-APCCy7 (1:100 dilution)	Becton Dickinson Biosciences	560654
Anti-Mouse CD14-FITC (1:200 dilution)	Biolegend	123311
Anti-Mouse/Human CD45R/B220-FITC (1:200 dilution)	Biolegend	103206
Anti-Human CD5-FITC (1:100 dilution)	Becton Dickinson Biosciences	555352
Anti-Human CD19-APC (1:100 dilution)	Becton Dickinson Biosciences	555415
Anti-Human CD19-BV421(HIB19) (1:100 dilution)	Biolegend	302233
Anti-Human TFEB (1:500 dilution)	Cell Signaling Technology	37785S
Anti-Human TBP (1:1000 dilution)	Cell Signaling Technology	8515S
Anti-Human BCL-XL (1:1000 dilution)	Cell Signaling Technology	54H6
Anti-Human BCL-2 (1:1000 dilution)	Becton Dickinson Biosciences	610539
Anti-Human MCL-1 (1:500 dilution)	Santa Cruz Biotech	SC-819
Anti-Human BCL-2A1 (1:1000 dilution)	Sigma-Aldrich	AV09047
Anti-Human NOXA (1:500 dilution)	Abcam	ab140129
Anti-Human PUMA (1:500 dilution)	Abcam	ab33906
Anti-Human BIM (1:500 dilution)	Becton Dickinson Biosciences	559685
Anti-Human p-ERK (1:1000 dilution)	Cell Signaling Technology	4370s
Anti-Human ERK (1:1000 dilution)	Cell Signaling Technology	9102s
Anti-Human p-JNK (1:1000 dilution)	Cell Signaling Technology	9251s
Anti-Human p-p38MAPK (1:1000 dilution)	Cell Signaling Technology	9211s
Anti-Human LAMP1 (1:1000 dilution)	Cell Signaling Technology	9091s
P-p42/44 MAPK (1:500 dilution)	Cell Signaling Technology	9101s
Anti-β–Actin (1:5000 dilution)	Sigma-Aldrich	A5441-.2ML
Anti-Mouse Lamp1–PE (1D4B) (1:100 dilution)	Santa Cruz Biotech	sc-19992-PE
Anti-Mouse Lamp2–Alexa488 (M3/84) (1:100 dilution)	Biolegend	108510

Biological Samples	Source	Catalog #
CLL Patient Samples (Project ID: 07/MRE05/44)	Cambridge University Hospitals - Addenbrookes	N/A
MCL Patient Samples (Project ID: 1894/07)	Technical University Munich	N/A
Patient-derived xenografts (Erasmus IRB)	University College London	N/A
Murine stromal cells	This paper	N/A
Chemical Compounds	**Source**	**Catalog #**
Zombie Aqua - BV510 (1:2000 dilution)	Biolegend	423101
Annexin-V FITC (1:50 dilution)	Biolegend	640945
DAPI (3 μM)	Biolegend	422801
Enzastaurin	Sigma-Aldrich	SML0762
Sotrastaurin	Selleck Chemicals	S2791
Bendamustine	Selleck Chemicals	S1212
Idelalisib	Selleck Chemicals	S2226
Midostaurin	Selleck Chemicals	S8064
Venetoclax	LC Labs	v-3579
Fludarabine	Cayman Chemicals	14128
Ibrutinib	SYNKinase	SYN-1171
Dexamethasone	Sigma-Aldrich	D4902
Vincristine Sulfate	Sigma-Aldrich	V8879
Critical Commercial Assays	**Source**	**Catalog #**
LEGENDplex Mouse Immunoglobulin Isotyping Panel	Biolegend	740492

REFERENCES

60. L. Wang, S. Wang, W. Li, RSeQC: quality control of RNA-seq experiments, *Bioinformatics* **28**, 2184–2185 (2012).

61. A. Dobin, C. A. Davis, F. Schlesinger, J. Drenkow, C. Zaleski, S. Jha, P. Batut, M. Chaisson, T. R. Gingeras, STAR: ultrafast universal RNA-seq aligner, *Bioinformatics* **29**, 15–21 (2013).

62. S. Anders, P. T. Pyl, W. Huber, HTSeq--a Python framework to work with high-throughput sequencing data, *Bioinformatics* **31**, 166–169 (2015).

63. M. I. Love, W. Huber, S. Anders, Moderated estimation of fold change and dispersion for RNA-seq data with DESeq2, *Genome Biol.* **15**, 550 (2014).

64. A. Sturn, J. Quackenbush, Z. Trajanoski, Genesis: cluster analysis of microarray data, *Bioinformatics* **18**, 207–208 (2002).

65. M. P. Weekes, S. Y. L. Tan, E. Poole, S. Talbot, R. Antrobus, D. L. Smith, C. Montag, S. P. Gygi, J. H. Sinclair, P. J. Lehner, Latency-associated degradation of the MRP1 drug transporter during latent human cytomegalovirus infection, *Science* **340**, 199–202 (2013).

66. E. J. Greenwood, N. J. Matheson, K. Wals, D. J. van den Boomen, R. Antrobus, J. C. Williamson, P. J. Lehner, Temporal proteomic analysis of HIV infection reveals remodelling of the host phosphoproteome by lentiviral Vif variants, *Elife* **5**, 12112 (2016).

67. R. Pan, L. J. Hogdal, J. M. Benito, D. Bucci, L. Han, G. Borthakur, J. Cortes, D. J. DeAngelo, L. Debose, H. Mu, H. Döhner, V. I. Gaidzik, I. Galinsky, L. S. Golfman, T. Haferlach, K. G. Harutyunyan, J. Hu, J. D. Leverson, G. Marcucci, M. Müschen, R. Newman, E. Park, P. P. Ruvolo, V. Ruvolo, J. Ryan, S. Schindela, P. Zweidler-McKay, R. M. Stone, H. Kantarjian, M. Andreeff, M. Konopleva, A. G. Letai, Selective BCL-2 inhibition by ABT-199 causes on-target cell death in acute myeloid leukemia, *Cancer Discov* **4**, 362–375 (2014).

68. N. L. M. Liem, R. A. Papa, C. G. Milross, M. A. Schmid, M. Tajbakhsh, S. Choi, C. D. Ramirez, A. M. Rice, M. Haber, M. D. Norris, K. L. MacKenzie, R. B. Lock, Characterization of childhood acute lymphoblastic leukemia xenograft models for the preclinical evaluation of new therapies, *Blood* **103**, 3905–3914 (2004).

DATA AVAILABILITY

The authors declare that the data supporting the findings of this study are available within the paper and its supplementary information.

The gene expression profile data have been deposited in the GEO database under accession numbers GSE119808 (CLL RNA-Seq, Figure 3) and GSE119813 (Stromal RNA-seq, Figure 4).

https://www.ncbi.nlm.nih.gov/geo/query/acc.cgi?acc=GSE119808

https://www.ncbi.nlm.nih.gov/geo/query/acc.cgi?acc=GSE119813

The mass spectrometry proteomics data have been deposited to the ProteomeXchange Consortium via the PRIDE partner repository with the dataset identifier PXD011062 and 10.6019/PXD011062.

https://www.ebi.ac.uk/pride/archive/projects/PXD011062

All other remaining data are available within the Article and Supplementary Files, or available from the authors upon request.